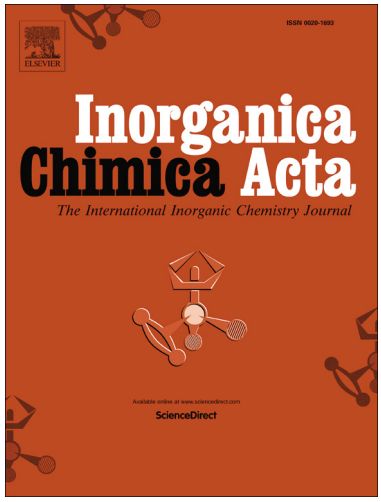

Synthesis and characterization of unique new lithium, sodium and potassium coordination polymers

Muhammad Nadeem, Moazzam H. Bhatti, Uzma Yunus, Mazhar Mehmood, Hafiz Muhammad Asif, Shoaib Mehboob, Ulrich Flörke

PII: S0020-1693(18)30231-7
DOI: https://doi.org/10.1016/j.ica.2018.04.045
Reference: ICA 18236

To appear in: *Inorganica Chimica Acta*

Received Date: 10 February 2018
Revised Date: 18 April 2018
Accepted Date: 22 April 2018

Please cite this article as: M. Nadeem, M.H. Bhatti, U. Yunus, M. Mehmood, H.M. Asif, S. Mehboob, U. Flörke, Synthesis and characterization of unique new lithium, sodium and potassium coordination polymers, *Inorganica Chimica Acta* (2018), doi: https://doi.org/10.1016/j.ica.2018.04.045

Synthesis and characterization of unique new lithium, sodium and potassium coordination polymers

Muhammad Nadeem[a,b], Moazzam H. Bhatti[a*], Uzma Yunus[a] , Mazhar Mehmood[b], Hafiz Muhammad Asif[c], Shoaib Mehboob[b], Ulrich Flörke[d]

[a] *Department of Chemistry, Allama Iqbal Open University, Islamabad, Pakistan*
[b] *National Center for Nanotechnology, Department of Metallurgy and Materials Engineering, Pakistan Institute of Engineering and Applied Sciences (PIEAS), Nilore 45650, Islamabad, Pakistan*
[c]*Department of Chemistry, Khwaja Fareed University of Engineering and Information Technology (KFUEIT), Rahim Yar Khan, Pakistan*
[d]*Anorganische und Analytische Chemie, Fakultät für Naturwissenschaften,Universität Paderborn, Warburgerstrasse 100, D-33098 Paderborn, Germany*

Abstract

Five new alkali metal coordination compounds [Li(NPG)](1a), $[Na(NPG)_2]\cdot 2H_2O$(2a), $[C_8H_5KO_4]$(3a), $[Li(NPA)_2H_2O]$(1b) and $[Na(NPA)_2]$(2b) wherein (NPG=N-phthaloyl glycine, NPA= N-phthaloyl-ß-alanine) have been synthesized and characterized by means of X ray single crystal analysis, Infrared spectroscopy (IR), Thermogravimetric analysis (TGA) and Florescence spectroscopy. The compounds 1a, 2a, 3a and 2b showed metal directed self-assembly supramolecular network structures. The crystal structure of compounds 1a and 1b showed distorted tetrahedral geometry with coordination number 4 around lithium. The carboxylate coordination modes were $\eta^2\mu^3$and $\eta^1\mu^1$ in 1a and 1b respectively. The compounds 2a and 2b exhibited distorted octahedral geometry with coordination number 6 around sodium. The carboxylate coordination mode in 2a and 2b is $\eta^2\mu^2$. The objective was to synthesize potassium complex [K(NPG)], but N-phthaloyl glycine was hydrolysed due to exothermic reaction in the presence of strong base, resulted, the formation of 3a. The multiple coordination modes of alkali metal ions to the carboxylate and ring carbonyl oxygen atoms of NPG and NPA produced unique three dimensional architectures. The compounds 1b and 2b showed two strong fluorescence emissions enhancement (blue emission maxima) with greater intensity comparative to NPA, while the compounds 1a and 2a showed two weak fluorescence emissions with less intensity comparative to ligand (NPG). The base hydrolysis of NPG with in the compound 3a resulted the

change of ligand based fluorochrome, which produced different shape emission spectrum as compared to other compounds.

Keywords: N-phthaloyl glycine; N-phthaloyl-ß-alanine; coordination polymer; X-ray; fluorescence spectroscopy.

1. Introduction

The most part of co-ordination chemistry is concerned with transition metal ions; however, S-block metal ions have attained generally little consideration. [1] Alkali or alkaline earth metal cations being non-dangerous and soluble in aqueous media are used in preference to coordinate with transition [2] or lanthanide [3] metal ions. The alkali and alkaline earth metal complexes are used in pharmaceuticals, [4] dyes, [5] and pigments [6]. The S-block cations have prime significance in solid-state structure and behave like a bridge in the intermolecular interactions. [7, 8] Alkali metal ions containing coordination polymeric structures are regularly less examined in detail. [9] In any case, this is a serious issue which is worth researching by keeping in mind the end goal to better comprehend the properties of these solid-state compounds. As linkers, carboxylates offer a variety of possible metal-binding motifs allowing for the formation of wide arrays of extended structures. [10-12] The development of various dimensional coordination polymer systems containing alkali or alkaline earth metal ions are predominantly taking into account due to anionic oxygen contributor. [13] The combination of alkali metal coordination polymers can be accomplished utilizing a salt and forming low-dimensional structures with neutral donor ligands, the later going about as synthetic scissors on the underlying material. [13] The basic differences of coordination polymers fundamentally influenced by the decision of the ligands, [14-16] metal ligand proportions, [17, 18]

solvents, [19-22] and counterions. [23] These variations produce wide range of self-assembled structures. [19-23] Mixed alkali and transition metal coordination polymer with 2, 6-Pyridinedicarboxylate produced robust structure with enhanced chemical and physical properties. [24, 25] The presence of two carbonyl groups with central nitrogen atom in Phthalimide derivatives [26] make them alluring to design supramolecular networks that find critical applications in catalytic reactions [27] and have been employed for the synthesis of chiral esters. [28] They have also used as biological probe as their fluorescence properties are highly environment sensitive. [29] The Phthalimide group acts as a protecting group for amines and amino acids. [30, 31] The N-protected amino acids are used for the synthesis of peptide bonds in the solid phase synthesis. [32]

Co-ordination chemistry of N-protected amino acids with metal ions is used to understand the coordination chemistry of proteins. [33] Many kinds of proteins within the body need metal ions to work, which can also be activated or deactivated by metal ions. These reversible reactions are caused by ligation of the metal ions and the proteins. If one has an understanding of the basic metal ion, N-protected α-amino acid complexation, then one could better identify the coordination site within the proteins. N-phthaloyl glycine has a variety of applications in medicinal chemistry, pharmaceuticals as dietary supplements, analytical and is used as antimicrobial reagents. [34]

In the present investigation we report the synthesis and luminescence properties of selected alkali metal compounds with NPG and NPA as ligands.

SCHEME OF WORK

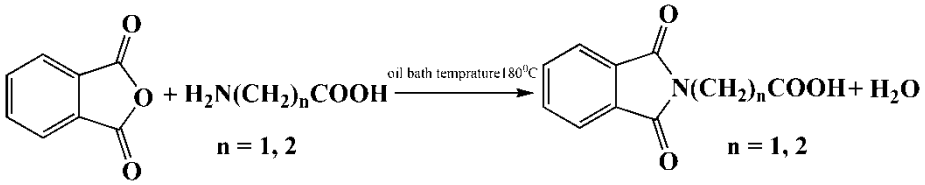

When n=1, N-phthaloyl glycine
n=2, N-Phthaloyl-Beta-Alanine

(a)

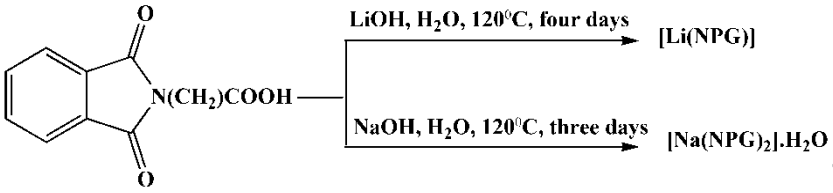

(b)

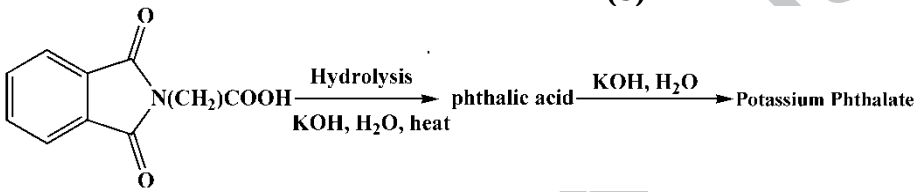

(c)

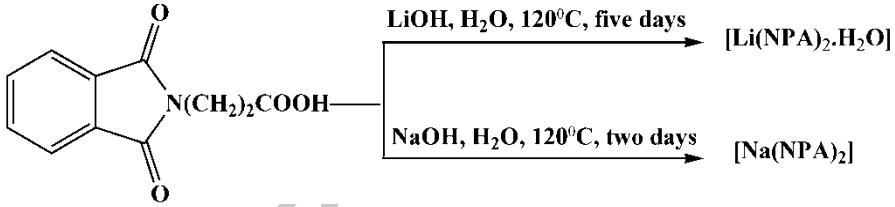

(d)

Scheme 1. Schematic illustration of the synthetic route for ligands (a) and complexes (1a and 2a) (b), 3a (c), and (1b and 2b) (d).

2. Experimental details

2.1. Reagents and Chemicals

NPG and NPA were prepared by the reported methods. [35] The synthesis scheme of ligands and complexes are presented in scheme 1. All solvents used for the synthesis were freshly distilled prior to use.

2.2. Instruments and Measurements

Nicolet iS 10 FTIR spectrophotometer was used to produce infrared spectra for all compounds in the range 4000-400 cm^{-1} through KBr discs. Melting points were determined via Gallen Kamp electro thermal apparatus, Cat No.MPD350, Sanyo, UK. Fluorescent emission spectra were recorded on F-7000 FL spectrophotometer 2133-007. Thermal decomposition patterns (TG and DTA) of all compounds were carried out under nitrogen atmosphere up to 800°C utilizing a heating rate of 10°C/min on a DTG-60H Simultaneous DTA-TG Analyzer. Raman spectroscopy was carried out using high resolution Raman spectroscopy system model MST 4000A (Germany). In Raman spectrometer main elements of setup are, laser sources 532 nm and 442 nm, samples slides and chamber light collection optics detection system.

2.3. Synthesis of 1a and 2a

An aqueous solution of metal (Li/Na) hydroxide (9.7mmol in 50ml) was added drop wise to well-stirred solutions of NPG (9.7mmol) in ethanol (40 ml) at room temperature separately. The pH of solution was adjusted to 6-7 and then stirred with heating (60 ºC) for next 3 hours, after that set aside for crystallization. After four weeks, 0.90g (43% yield) for 1a and 0.85g (18% yield) for 2a of colourless single crystals of good quality were obtained.

2.4. Synthesis of 3a

An aqueous solution of potassium hydroxide (9.8mmol in 50ml) was added drop wise to a well-stirred solution of NPG (9.8mmol) in ethanol (40 ml) at room temperature. The solution was stirred for next 4 hours with heating. Due to intense heat the base hydrolysis of NPG had occurred [36] and phthalic acid is formed as an intermediate product. This phthalic acid reacted with KOH to form colourless crystals of potassium phthalate confirmed by single X-rays crystal analysis.

2.5. Synthesis of 1b and 2b

An aqueous solution of metal (Li/Na) carbonate (4.5mmol in 50ml) was added drop wise to a well-stirred solution of NPA (9.1mmol) in ethanol (40 ml) at room temperature separately. The pH (6-7) adjusted solution was stirred with heating (60 ºC) for next 4 hours and then set aside for crystallization. After four weeks, 0.48g (48% yield) for each 1b and 2b of colourless single crystals were obtained.

3. Results and Discussion

The physical characteristics of the synthesized compounds are given in Table 1.

Table 1. Physical properties data of the compounds 1a, 2a, 3a, 1b and 2b.

Compounds	Formula	M.P (°C)	%Yield
1a	$C_{10}H_6NO_4Li$	320	43
2a	$C_{20}H_{17}N_2O_{10}Na$	298	18
3a	$C_8H_5O_4K$	<340	20
1b	$C_{22}H_{19}N_2O_9Li$	300	48
2b	$C_{22}H_{17}N_2O_8Na$	258	48

3.1. Infrared and Raman spectra

FTIR spectra of all compounds were registered in the KBr matrix presented in Fig. 1(a) and Table 2. The Raman spectra were taken in the range of 2000-150 cm^{-1} showed in Fig. 1(b). The very broad band at 3568 cm^{-1} appeared due to stretching frequency ν(OH) of acid appeared in the spectrum of free N-phthaloyl glycine disappeared in the spectra of its compounds 1a and 2a confirmed that, the hydrogen ion of carboxylate group of free N-phthaloyl glycine was substituted by the metal ions by de-protonation. [33] IR spectrum of 1a and 2b showed in Fig. 1 devoid of any absorption beyond 3310 cm^{-1}, which clearly indicates the absence of any sort of water molecule [1] in the compounds 1a and 2b, the sharp absorption observed at 3476 cm^{-1} in the compound 2a indicates the presence of lattice water molecule, medium broad absorption observed for 1b at 3413 cm^{-1} proves the

presence of coordinated water molecule. [37-39] The bands at 3128 (O-H stretch) and 1718 cm^{-1} (C=O) for 1b indicate that one of the carboxylate groups remains protonated. The O-H stretch for 3a is present at 3127 cm^{-1} confirmed the presence of protonated carboxyl group. The ring carbonyl single band of N-phthaloyl moiety for ligands (NPG &NPA) and compounds 1a, 2a, 1b and 2b appeared in the range 1779-1770 cm^{-1} (IR_{KBr}), 1755-1779 (Raman), while absent for 3a. This confirms the hydrolysis of NPG in 3a. The Raman spectra peaks at 1715 cm^{-1} for 2a, 1703 cm^{-1} for 1b and 2b attributed to the stretching vibration of carboxyl group (C=O) while absent for 1a and 3a. [39] The corresponding stretching vibration for IR are 1732 cm^{-1} for NPG, 1731 cm^{-1} for 1a, 1720 cm^{-1} for 2a, 1717 cm^{-1} for 3a, two peaks at 1722 cm^{-1} and 1705 cm^{-1} for NPA, 1718 cm^{-1} for 1b, 1716 cm^{-1} for 2b. The characteristic asymmetric (ma) and symmetric (ms) stretches due to the carboxylate group (COO^{-1}) are as follows. [39]

1628 cm^{-1} and 1401 cm^{-1} (IR_{KBR}), absent in Raman for 1a

1465 cm^{-1} and 1319 cm^{-1}(IR_{KBR}), 1600 cm^{-1} and 1409 cm^{-1} (Raman) for 2a

1559 cm^{-1} and 1399 cm^{-1}, (IR_{KBR}), 1588 cm^{-1} and 1484 cm^{-1} (Raman) for 3a

1617 cm^{-1} and 1400cm^{-1}, (IR_{KBR}), 1600 cm^{-1} and 1182 cm^{-1} (Raman) for 1b

1608 cm^{-1} and 1321 cm^{-1}, 1600 cm^{-1} and 1179 cm^{-1} (Raman) for 2b.

Table 2. Infrared (cm^{-1}) spectral data of compounds 1a, 2a, 3a, 1b and 2b.

Compounds	ν(OH) carboxylic	ν(OH) lattice water	ν(OH) coordinated water	ν(C=O) carboxylic	ν(C=O) carbonyl	νas(COO-)	νsy(COO-)	ν(C-OH)	δ(C-OH)	ν(M-O)
NPG	3568	-	-	1732	1770	-	-	1217	994	-
1a	-	-	-	1731	1779	1628	1401	-	-	567, 582
2a	-	3476	-	1720	1775	1465	1319	-	-	534, 599
3a	3127	-	-	1717	-	1559	1399	1264	1078	442
NPA	3206	-	-	1722, 1705	1770	-	-	1212	1001	-
1b	3128	-	3413	1718	1772	1617	1400	1230	1010	531
2b	-	-	-	1716	1770	1608	1321	-	-	532

ν = stretching,δ= bending, as = asymmetrical, sy=symmetrical

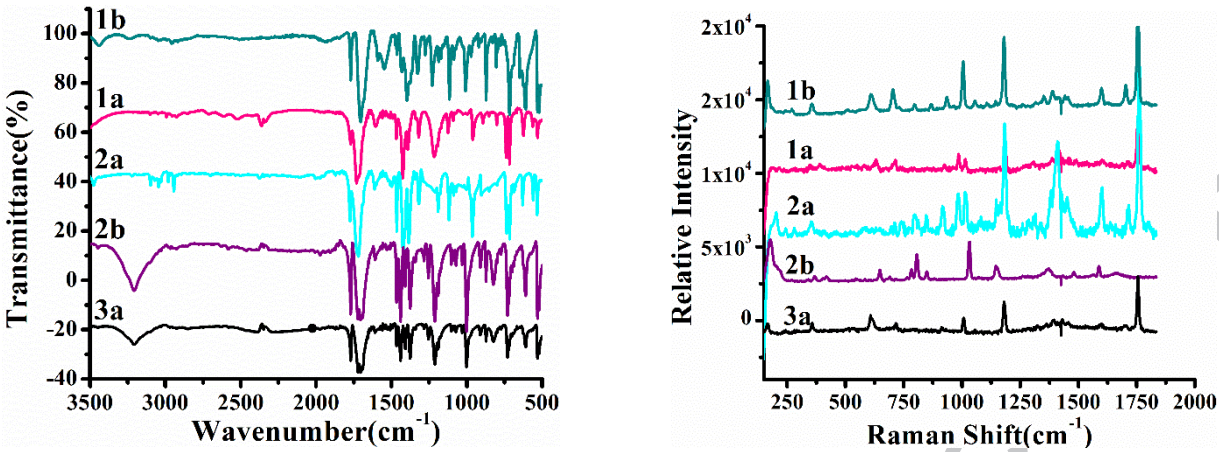

Fig. 1. FTIR spectra (a) and Raman spectra (b) of compounds 1a, 2a, 3a, 1b and 2b.

3.2. Crystal Structure Description of compounds

3.2.1. Structure Determination

The intensity data for all compounds were recorded using a Bruker SMART CCD area-detector diffractometer with graphite monochromatic MoK_α radiation (λ = 0.71073 Å) at T = 130(2) K. Semi-empirical absorption correction applied from equivalent reflections. Structure solutions were obtained by direct methods [40] and refined through full-matrix least squares refinements [40] based on F^2. All atoms expect hydrogen were refined an-isotropically, H-atoms were clearly located from difference fourier maps, refined at idealized positions riding on the parent atoms with isotropic displacement parameters $U_{iso}(H)$ = $1.2U_{eq}(C/O)$ and C-H 0.95-0.98 Å. Specific crystal data and structure refinement details are given in Table 3, selected bond lengths as well as selected bond angles are given in Table 4 and 5 respectively.

3.2.2. Specific structural details of 1a

Single crystal X-ray diffraction analysis, revealed the formation of the lithium compound $[C_{10}H_6NO_4Li]$ (1a). Each lithium atom (Fig. 2a) is coordinated by three carboxylate

oxygen atoms [O(3), O(3B), O(4B)] in a bridging mode and one carbonyl oxygen atom [O(1A)]. The selected bond angles(deg): O(3)-Li(1)-O(4)#1, 109.57º(14); O(3)-Li(1)-O(3)#2, 113.88º(14); O(4)#1-Li(1)-O(3)#2, 111.96º(16); O(3)-Li(1)O(1)#3, 103.92º(15); O(4)#1-Li(1)-O(1)#3, 110.66º(14); O(3)#2-Li(1)-O(1)#3, 106.51º(14) suggested the formation of slightly distorted tetrahedral geometry of Lithium compound with coordination number 4. The two carbonyl groups present in NPG behaved differently, one group with bond length 1.209(2) Å coordinated with metal while other (1.207(2)) remains uncoordinated. The carboxylate bond lengths are 1.256(2) Å & 1.239(2) Å for O(3)-C(10), O(4)-C(10) respectively with coordination mode $\eta^2\mu^3$.[41] The bond length between lithium and oxygen is different for different motifs. The bond lengths [Li(1)-O(3) 1.909(3) Å], [Li(1)-O(4A) 1.909(3) Å], [Li(1)-O(3B) 1.918(3) Å], [Li(1)-O(1A) 1.936(3)Å] indicate that the carbonyl oxygen atom makes weaker bond with lithium as compared to the carboxylate oxygen atoms. Further the compound 1a crystallized in the non-centrosymmetric space group P 2(1); however, the absolute configuration cannot be determined due to the absence of anomalous scattering effects. The schematic diagram of the coordination behaviour of lithium in compound 1a is shown in Fig. 2b. The lithium metal directed self-assembly (Fig. 2c) produced unique supramolecular structure.

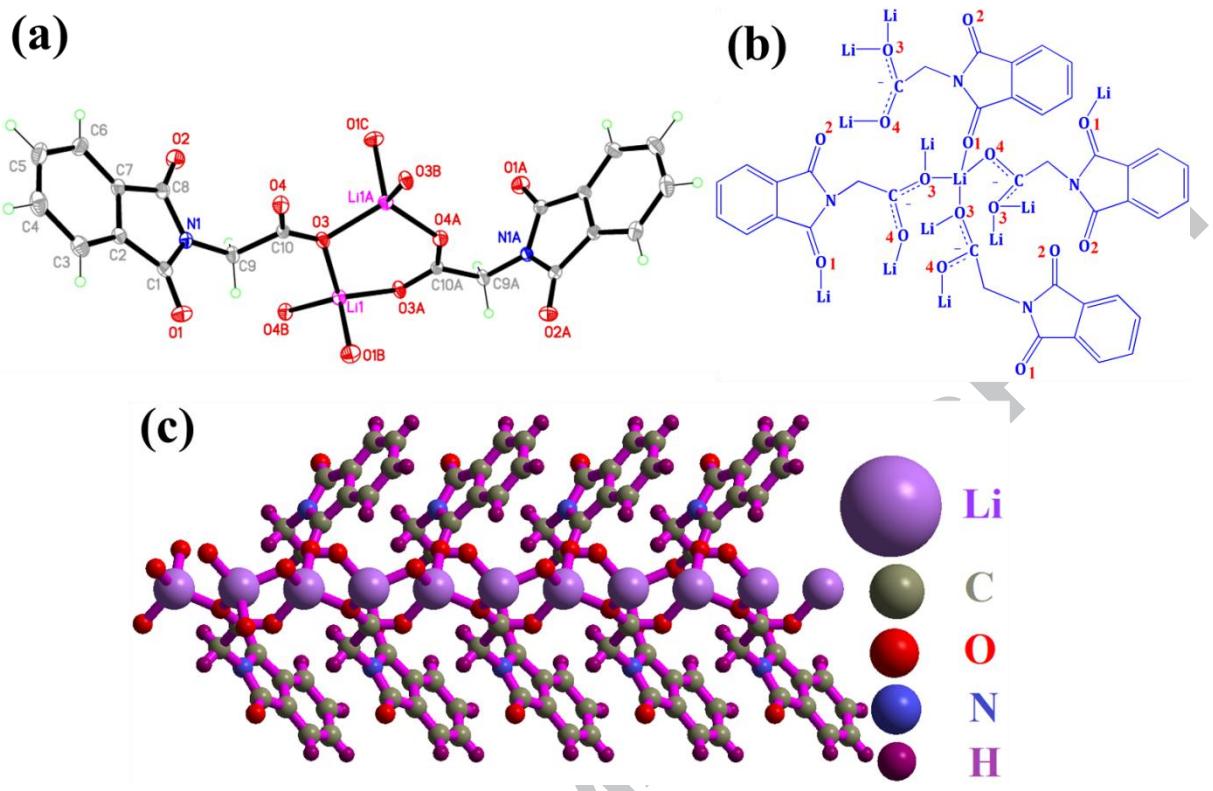

Fig. 2. (a) View of the molecular structure of LiNPG (1a) showing the coordination geometry about Lithium, anisotropic displacement ellipsoids are drawn at the 50% probability level (colour codes: Li, pink; C, grey; O, red; N, blue; H, green), symmetry transformations used to generate equivalent atoms for 1a: #1, x, y-1, z; #2, -x+1, y-1/2, -z+1; #3, -x+2, y-1/2, -z+1; #4, -x+1, y+1/2, -z+1; #5, -x+2, y+1/2, -z+1; #6, x, y+1, z. (b) Schematic diagram of the coordination behaviour of lithium in compound 1a. (c) Self-assembly diagram along a axis of 1a.

3.2.3. Specific structural details of 2a

Single-crystal X-ray diffraction analysis, showed the formation of the sodium compound $[C_{20}H_{13}N_2O_8Na].2H_2O$ (2a). Each sodium atom is coordinated by four carboxylate oxygen atoms [O(3), O(3C), O(4D), O(4E)] in a bridging mode and two carbonyl oxygen atoms [O(1A), O(1B)] presented in Fig. 3a. The measured bond distance for O3-C10 is 1.227(2) Å and for O4-C10 is 1.291(2) Å in single crystallographically independent ligand NPG, the difference is significant and might indicate that O4 is hemiprotonated. This supposition is also supported by the fact that the compound was crystallized in acidic environment (pH 6-7). Indeed it was not possible to derive meaningful and eventual O-H positions from the difference maps. The selected bond angles (deg) suggested the formation of distorted octahedral

geometry with coordination number 6. The two carbonyl groups showed the similar behaviour as in 1a, but here the difference of C-O bond length for metal coordinated (1.212(2) Å) and uncoordinated (1.206(2) Å) is much more evident than 1a. The carboxylate coordination mode is $\eta^2\mu^2$ bridging. Two solvent water molecules are present per formula unit. The schematic diagram of the coordination behaviour of sodium in compound 2a and supramolecular structure is shown in Fig. 3b and 3c.

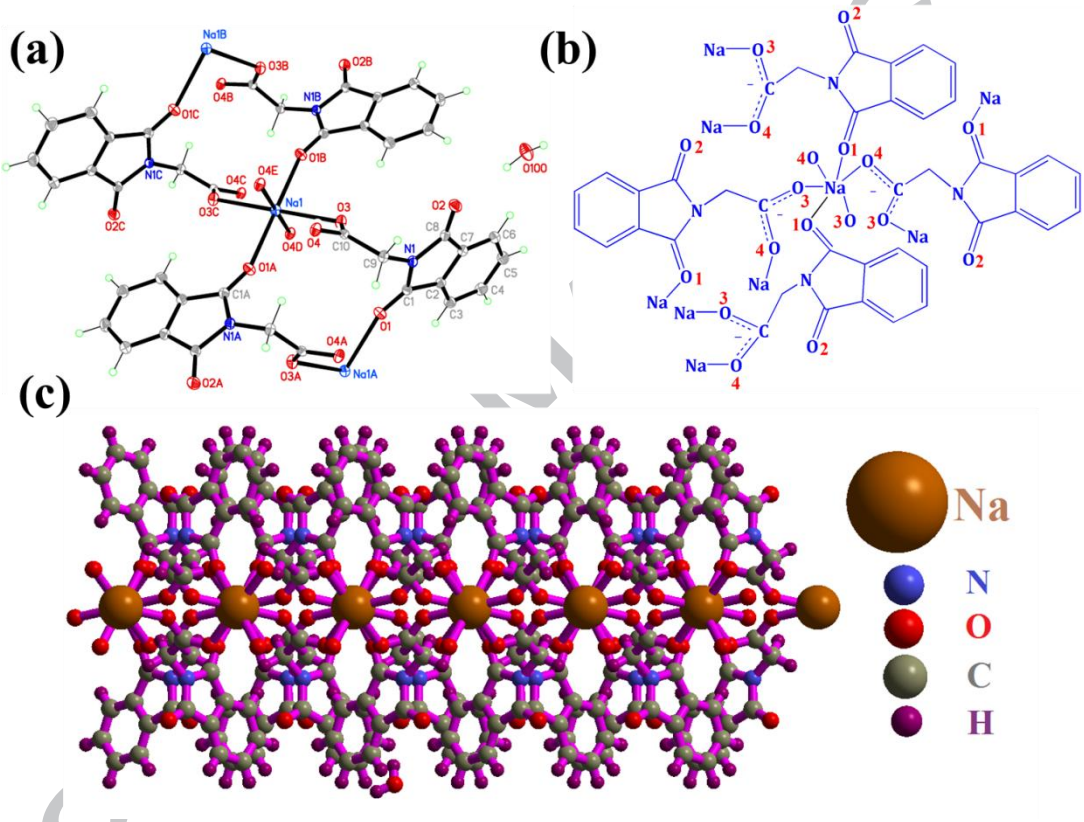

Fig. 3. (a) View of the coordination environment of Na for NaNPG (2a), anisotropic displacement ellipsoids are drawn at the 50% probability level (colour codes: Na, blue; C, grey; O, red; N, blue; H, green), symmetry transformations used to generate equivalent atoms for 2a: #1, -x, -y+1, -z+2; #2, x, y-1, z; #3, -x, -y, -z+2; #4, x, -y, z-1/2; #5, -x, y, -z+5/2; #6, x, y+1, z. (b) schematic diagram of the coordination behaviour of sodium in compound 2a. (c) Self-assembly diagram along c* axis of 2a.

3.2.4. Specific structural details of 3a

Single crystal X-ray diffraction analysis, confirmed the formation of the potassium compound [$C_8H_5O_4K$] (3a) (Fig. 4a). The co-ordination number of K is 7 with pentagonal bipyramidal (Fig. 4b). The self-assembly is evident in Fig. 4c.

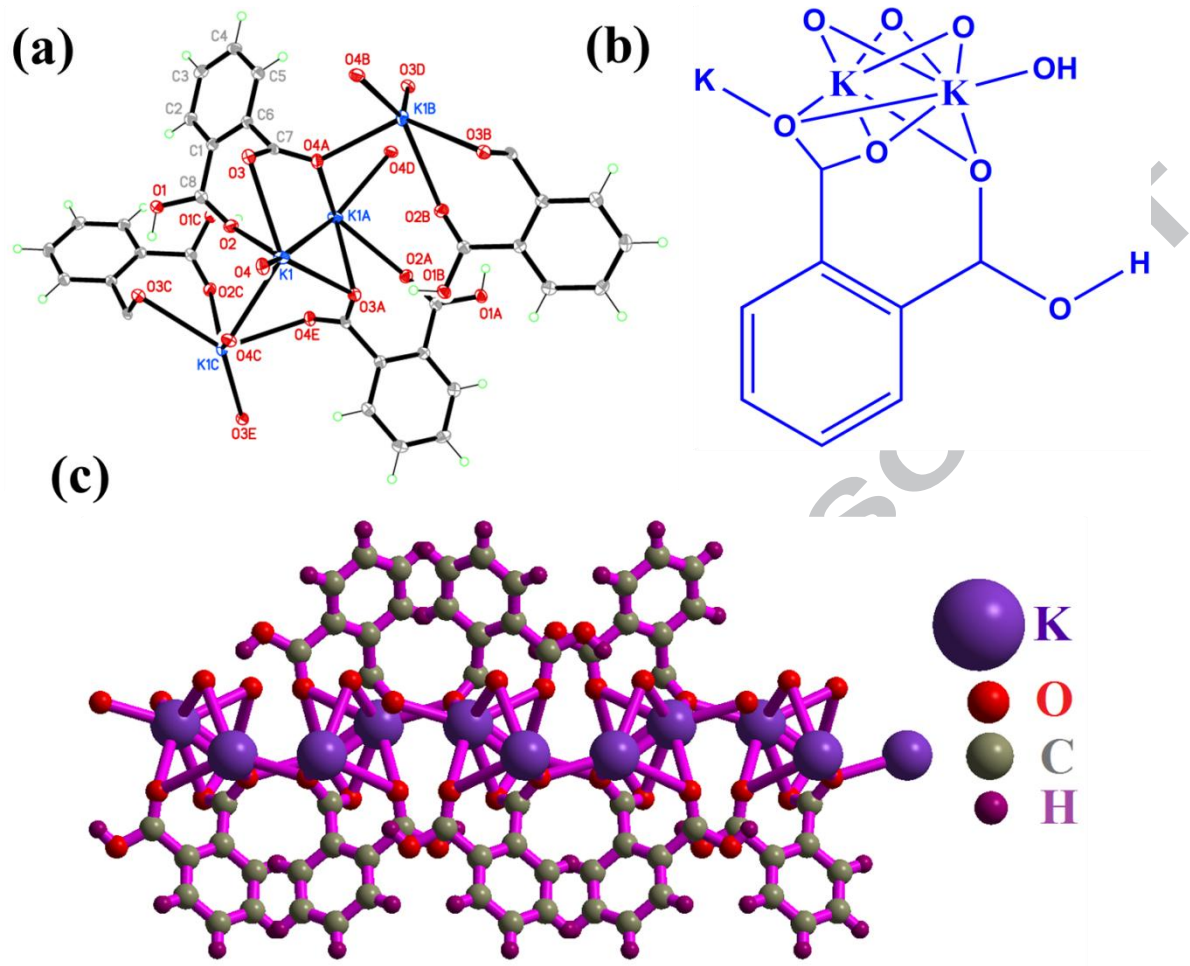

Fig. 4. (a) View of the molecular structure of 3a showing the coordination geometry about potassium, anisotropic displacement ellipsoids are drawn at the 50% probability level, (colour codes: K, blue; C, grey; O, red; H, green), symmetry transformations used to generate equivalent atoms for 3a: #1, -x+1/2, y, z-1/2; #2, -x, -y, z-1/2; #3, -x, -y, z+1/2; #4, -x+1/2, y, z+1/2. (b) Schematic diagram of the coordination behaviour of sodium in compound 3a. (c) Self-assembly of 3a along b* axis.

3.2.5. Specific structural details of 1b and 2b

The single crystal X-ray diffraction displayed the formation of lithium compound [$C_{22}H_{17}N_2O_8Li.H_2O$] (1b) and [$C_{22}H_{17}N_2O_8Na$] (2b). The structural details of 1b is described as, each lithium atom is coordinated by four oxygen atoms labelled as O(4), O(5), O(8) and O(9) which are related to the three NPA ligands and one water molecule shown in Fig. 5(a) along with schematic view in Fig. 5 (b). The carboxy oxygen atoms O(4) and O(8) are related to two different crystallographically independent NPA ligands. One NPA ligand which is coordinated to Li(I) ion through O(4) has been refined in protonated form,

the bond length difference between C11-O3 (1.310(2) Å) and C11-O4 (1.211(2) Å) is evident, suggesting the protonation of O(3) as O(3)-H(3)). The second carboxy group oxygen O(8) coordinated to Li (I) ion is related to the other crystallagraphic independent deprotonated NPA ligand, bond distances C22-O7 and C22-O8 of the deprotonated carboxy group are nicely the same. The ring carbonyl O(5) atom related to deprotonated NPA ligand also connected to Li(I) ion through the third coordination bond around lithium. The bond length is mentioned here for two ring carbonyl of deprotonated NPA, one is coordinated C12-O5 (1.216Å) and other is uncoordinated C19-O6 (1.210(2) Å). One coordinated water molecule having O(9) atom refined as neutral ligand forming forth coordination bond with Li(I) ion. The selected bond angles (deg) suggest the formation of distorted tetrahedral geometry with coordination number 4 around lithium. The carboxylate coordination mode is $\eta^1\mu^1$. For 2b one crystallographically independent NPA ligand is refined, but from molecular formula the metal to ligand ratio found is 1:2, also there is reasonable difference in the bond distance of C11-O3 (1.226 Å) and C11-O4 (1.291Å) relating to carboxy group of refined NPA, the third important fact is that 2b was crystallized in acidic pH (6-7) environment. All aforementioned facts support the claim that ligand NPA is not fully deprotonated but it is hemiprotonated. The crystallographic limits can be understood as previously discussed in the crystallographic discussion part of compound 2a. Each sodium atom in 2b is coordinated by four carboxylate oxygen atoms [O(3B), O(3C), O(4B), O(4C)] in a bridging mode and two ring carbonyl oxygen atom [O(1), O(1A)] (see Fig. 5c) producing self-assembly structure shown in Fig. 6e. The selected bond angles (deg) suggest the formation of distorted octahedral geometry with coordination number 6. The two carbonyl groups present in n-phthaloyl **ß-**alanine behave

differently as O(1) coordinates to Na while O(2) remains uncoordinated. The carboxylate coordination mode is $\eta^2\mu^2$ bridging. The schematic diagram of 2b is present in Fig. 5d.

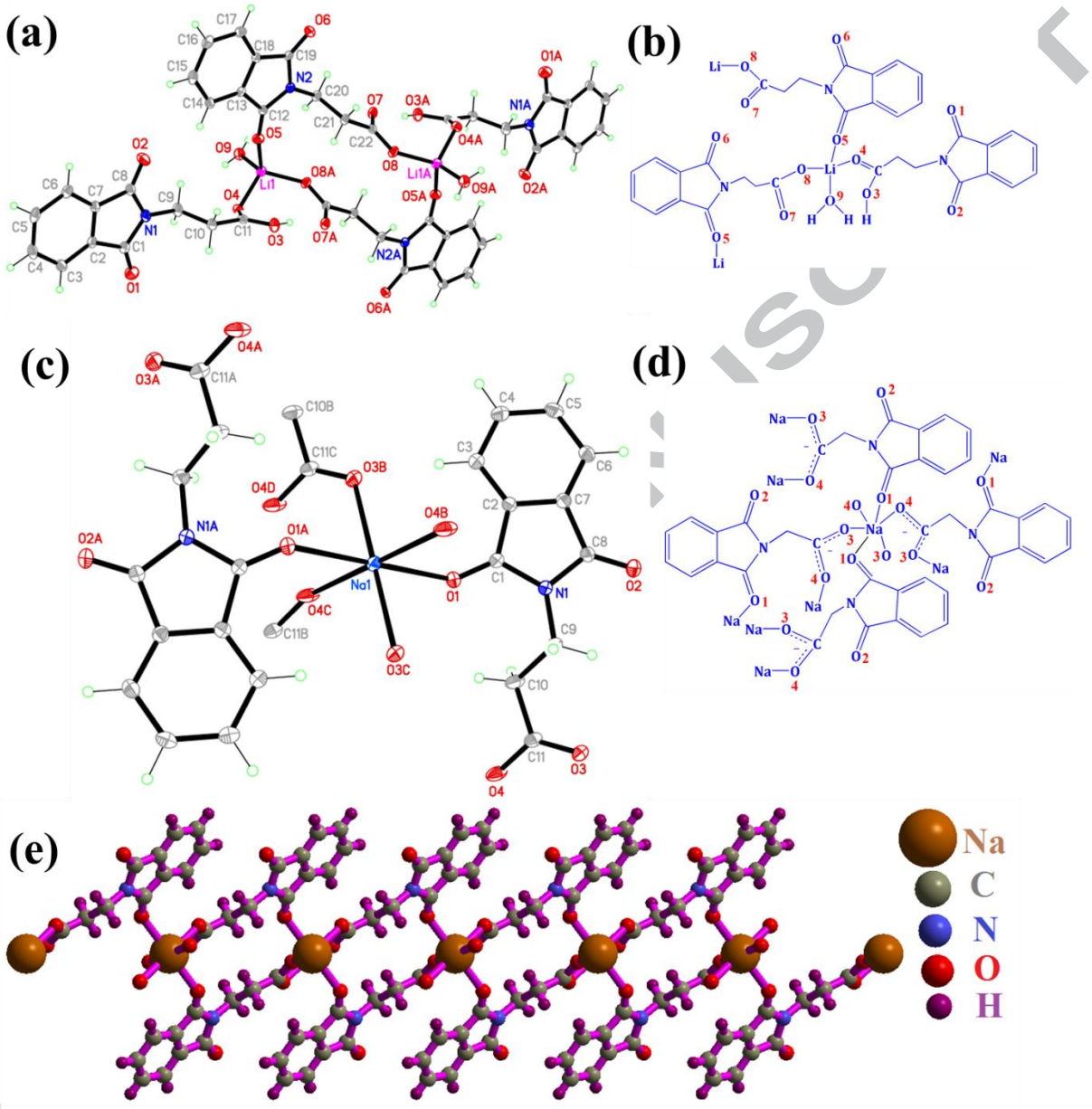

Fig. 5. The coordination environment of Li(I) ion for compound 1b (a) and Na(I) ion for compound 2b (c), anisotropic displacement ellipsoids are drawn at the 50% probability level, (colour codes: Li, pink; C, grey; O, red; N, blue; H, green for 1b and Na, blue; C, grey; O, red; N, blue; H, green for 2b), symmetry transformations used to generate equivalent atoms: #1, -x+2, -y+1, -z+1 for 1b and #1, x, y-1, z; #2, -x+2, -y+2, -z; #3, x-1, y-1, z; #4, -x+3, -y+2, -z; #5, -x+2, -y+1, -z; #6, x+1, y+1, z; #7, x, y+1, z for 2b. (b) and (d) Schematic diagram of the coordination behavior of lithium and sodium respectively. (e) Self-assembly of 2b along b axis using ball and stick model.

Table 3. Crystal data and structure refinement details of compounds for 1a, 2a, 3a, 1b and 2b.

	1a	2a	3a	1b	2b
Empirical formula	C_{10} H_6 Li N O_4	C_{20} H_{17} N_2 Na O_{10}	C_8 H_5 K O_4	C_{22} H_{19} Li N_2 O_9	C_{22} H_{17} N_2 Na O_8
Formula weight	211.1	467.34	204.22	462.33	459.36
T (K)	130(2)	130(2)	130(2)	130(2)	130(2)
Wavelength (Å)	0.71073	0.71073	0.71073	0.71073	0.71073
Crystal system	Monoclinic	Orthorhombic	Orthorhombic	Triclinic	Monoclinic
Space group	P2(1)	Pbcn	Pca2(1)	P-1	P2(1)/n
a (Å)	7.2750(19)	33.517(3)	9.5684(9)	6.9625(6)	5.2397(4)
b (Å)	4.8795(13)	5.0923(5)	13.2423(12)	10.3480(9)	7.0386(6)
c (Å)	13.416(4)	11.9039(11)	6.4190(6)	15.8169(13)	27.744(2)
α (°)	90	90	90	102.721(2)	90
β (°)	98.259(5)	90	90	98.527(2)	91.792(2)
γ (°)	90	90	90	100.575(2)	90
Volume ($Å^3$)	471.3(2)	2031.7(3)	813.34(13)	1071.36(16)	1022.68(14)
Z	2	4	4	2	2
D calc (Mg/m^3)	1.488	1.528	1.668	1.433	1.492
Absorption coefficient(mm^{-1})	0.115	0.142	0.627	0.112	0.133
F(000)	216	968	416	480	476
Crystal size (mm^3)	0.48 x 0.22 x 0.19	0.48 x 0.33 x 0.25	0.38 x 0.20 x 0.10	0.47 x 0.21 x 0.11	0.48 x 0.20 x 0.12
θ(°) range	1.53 to 27.88	2.43 to 27.88	1.54 to 27.87	2.07 to 27.88	1.47 to 27.86
Reflections collected	4497	17568	6954	10271	9219
Independent reflections	1257	2419	1921	5081	2441
R(int)	0.0176	0.0244	0.0208	0.0212	0.0222
Completeness to θ = 27.88°	99.90%	0.999	0.998	99.60%	100.00%
Max. and min. transmission	0.9785 and 0.9469	0.9654 and 0.9351	0.9399 and 0.7966	0.9878 and 0.9493	0.9843 and 0.9391
CCDC Number	870359	870722	872685	873800	876492

Table 4. Selected metal-oxygen bond distances (Å) for 1a, 2a, 3a, 1b and 2b.

1a (M-O)& (M-M)	Bond Distance(Å)	2a (M-O)	Bond Distance(Å)	3a (M-O)	Bond Distance(Å)	1b(M-O)	Bond Distance(Å)	2b (M-O)	Bond Distance(Å)
Li(1)-O(3)	1.909(3)	Na(1)-O(4)#1	2.2946(9)	K(1)-O(4)#1	2.6271(11)	Li(1)-O(8)#1	1.900(3)	Na(1)-O(4)#1	2.3065(11)
Li(1)-O(4)#1	1.909(3)	Na(1)-O(4)#2	2.2946(9)	K(1)-O(4)	2.7441(13)	Li(1)-O(9)	1.903(3)	Na(1)-O(4)#2	2.3065(11)
Li(1)-O(3)#2	1.918(3)	Na(1)-O(3)#3	2.3797(9)	K(1)-O(3)	2.7724(11)	Li(1)-O(4)	1.938(2)	Na(1)-O(3)#3	2.3668(11)
Li(1)-O(1)#3	1.936(3)	Na(1)-O(3)	2.3797(10)	K(1)-O(3)#2	2.7875(11)	Li(1)-O(5)	1.960(2)	Na(1)-O(3)#4	2.3668(11)
Li(1)-Li(1)#2	3.032(3)	Na(1)-O(1)#4	2.4130(10)	K(1)-O(2)	2.8501(11)	O(8)-Li(1)#1	1.900(3)	Na(1)-O(1)	2.4347(11)
Li(1)-Li(1)#4	3.032(3)	Na(1)-O(1)#5	2.4130(10)	K(1)-O(4)#2	2.9648(11)	----------	----------	Na(1)-O(1)#5	2.4347(11)
O(1)-Li(1)#5	1.936(3)	O(1)-Na(1)#5	2.4130(10)	K(1)-O(2)#3	3.1076(12)	----------	----------	Na(1)-O(4)#1	2.3065(11)
O(3)-Li(1)#4	1.918(3)	O(4)-Na(1)#6	2.2946(9)	O(2)-K(1)#2	3.1076(12)	----------	----------	O(3)-Na(1)#6	2.3668(11)

Table 5. Bond angles (deg) around the metal centres for 1a, 2a, 3a, 1b and 2b.

	BOND ANGLES(°)	2a	BOND ANGLES(°)	3a	BOND ANGLES(°)	1b	BOND ANGLES(°)	2b	BOND ANGLES(°)
O(3)-Li(1)-O(4)#1	109.57(14)	O(4)#1-Na(1)-O(4)#2	180.0	O(4)#1-K(1)-O(4)	89.23(3)	O(8)#1-Li(1)-O(9)	106.43(12)	O(4)#1-Na(1)-O(4)#2	180.00(7)
O(3)-Li(1)-O(3)#2	113.88(14)	O(4)#1-Na(1)-O(3)#3	95.00(3)	O(4)#1-K(1)-O(3)	129.53(3)	O(8)#1-Li(1)-O(4)	112.11(12)	O(4)#1-Na(1)-O(3)#3	95.92(4)
O(4)#1-Li(1)-O(3)#2	111.96(16)	O(4)#2-Na(1)-O(3)#3	85.00(3)	O(4)-K(1)-O(3)	87.00(3)	O(9)-Li(1)-O(4)	115.59(12)	O(4)#2-Na(1)-O(3)#3	84.08(4)
O(3)-Li(1)-O(1)#3	103.92(15)	O(4)#1-Na(1)-O(3)	85.00(3)	O(4)#1-K(1)-O(3)#2	89.37(4)	O(8)#1-Li(1)-O(5)	115.47(12)	O(4)#1-Na(1)-O(3)#4	84.08(4)
O(4)#1-Li(1)-O(1)#3	110.66(14)	O(4)#2-Na(1)-O(3)	95.00(3)	O(4)-K(1)-O(3)#2	132.82(3)	O(9)-Li(1)-O(5)	111.38(12)	O(4)#2-Na(1)-O(3)#4	95.92(4)
O(3)#2-Li(1)-O(1)#3	106.51(14)	O(3)#3-Na(1)-O(3)	180.00(3)	O(3)-K(1)-O(3)#2	127.75(3)	O(4)-Li(1)-O(5)	95.98(11)	O(3)#3-Na(1)-O(3)#4	180.0
O(3)-Li(1)-Li(1)#2	133.08(16)	O(4)#1-Na(1)-O(1)#4	102.50(3)	O(4)#1-K(1)-O(2)	82.77(3)	----------	----------	O(4)#1-Na(1)-O(1)	79.82(5)
O(4)#1-Li(1)-Li(1)#2	74.62(9)	O(4)#2-Na(1)-O(1)#4	77.50(3)	O(4)-K(1)-O(2)	137.88(3)	----------	----------	O(4)#2-Na(1)-O(1)	100.18(5)
O(3)#2-Li(1)-Li(1)#2	37.50(10)	O(3)#3-Na(1)-O(1)#4	90.87(3)	O(3)-K(1)-O(2)	67.68(3)	----------	----------	O(3)#3-Na(1)-O(1)	94.63(4)
O(1)#3-Li(1)-Li(1)#2	118.49(15)	O(3)-Na(1)-O(1)#4	89.13(3)	O(3)#2-K(1)-O(2)	88.55(3)	----------	----------	O(3)#4-Na(1)-O(1)	85.37(4)
O(3)-Li(1)-Li(1)#4	37.70(4)	O(4)#1-Na(1)-O(1)#5	77.50(3)	O(4)#1-K(1)-O(4)#2	147.96(4)	----------	----------	O(4)#1-Na(1)-O(1)#5	100.18(5)
O(4)#1-Li(1)-Li(1)#4	136.81(17)	O(4)#2-Na(1)-O(1)#5	102.50(3)	O(4)-K(1)-O(4)#2	118.76(4)	----------	----------	O(4)#2-Na(1)-O(1)#5	79.82(5)

3.3. Thermal stability studies

Thermal analysis curves of all studied compounds are shown in Fig. 6. The thermo analytical data is summarized in Table 6. The thermal analyses of compound 1a does not show any weight loss up to 230°C indicating the absence of any coordinated or lattice water molecules in the complex.[44] Its thermal degradation occurred in two steps. These two steps in the range of temperature 230-470°C & 470-805°C showed the decomposition of NPG. [45] These two stages are in connection with a weight loss of 90.90%. The calculated weight loss value in these two stages is 92.85%. The total observed weight loss value is 90.90% with a residue equal 9.1% which is corresponding to lithium oxide Li_2O.[46] These results show good agreement with the theoretical values of total loss equal 92.85% and residual 7.11%.

Table 6. Thermal data of compounds 1a, 2a, 3a, 1b and 2b.

Compounds/ Codes	**Number of Stages**	**Temp. range (^{o}C)**	**$T_{max.}$ (^{o}C)**	**Thermogravimetry(TG)**			**Decomposition Species**
				Mass Loss (%) Observed		**Mass Loss (%) calculated**	
1a	2	230-470 470-805	426 (-) 709(-)	40.45 50.32	90.90	92.85	NPG
2a	6	60-115 116-176	80(+) 126(+)	3.107 3.950	7.057	7.71	$2H_2O$
		177-254 255-345 346-389 390-650	204(+) 308(+) 364(+) 472(-)	40.337 24.416 8.960 7.852	82.41	83.87	2NPG
3a	3	250-350 351-572 573-750	313(+) 525(-) 747(-)	40.938 13.896 12.850	67.68	65.23	Phthalic acid
1b	5	100-140	118 (+)	4.05	3.90	H_2O	100-140
		141-170 171-292 293-400 401-775	155(+) 275(+) 338(-) 642(-)	0.527 44.023 25.273 21.62	91.44	92.79	141-170 171-292 293-400 401-775
2b	2	200-450 451-790	269(+) 594(-)	67.351 21.608	89.48	91.43	2NPA

The TG-DTA curves of 2a indicate six step decompositions. Dehydration of two water molecules is observed endothermally in the first two steps between 60-115°C and 116-176°C.[47] The rest four stages in the range of 177-650°C showed decomposition of two NPG. These four stages are in connection with a weight loss of 82.41%. The calculated weight loss value in these four stages is 83.87%. The total observed weight loss value is 89.47 % with a residue equal 10.53 % corresponds to sodium peroxide. These results show good agreement with the theoretical values of total weight loss equal to 91.57% and residual 8.35%.

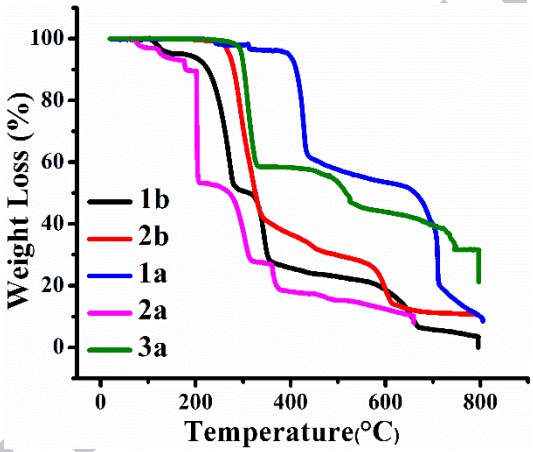

Fig. 6. TGA curves of compounds 1a, 2a, 3a, 1b and 2b.

The thermal analyses of compound 3a does not show any weight loss up to 250°C indicating the absence of any coordinated or lattice water molecules in the complex. Its thermal degradation occurred in three stages in the range from 250-750°C giving potassium super oxide as a final residue.[48] The total weight loss value was 67.68% with a final residue 32.3% which is equivalent to the theoretical values 65.23% and 34.77%, respectively. The TG-DTA curves of 1b indicate five step decompositions. Dehydration of one water molecules is observed endothermally in the first step between 100-140°C. The rest four stages range of 141-775°C showed the decomposition of two NPA.[49]

These four stages are in connection with a weight loss of 91.44% and the calculated weight loss value in these four stages is 92.79%. The total observed weight loss value is 95.53% with a residue equal 4.05% corresponds to lithium oxide Li_2O. These results show good agreement with the theoretical values, total loss equal 96.68% and residual 3.89%. The thermal degradation of 2b occurred in two stages in the range from 200-450°C and 451-790°C giving sodium peroxide (Na_2O_2) as a final residue.[48] The total weight loss value was 89.48% with a final residue 10.52% which is equivalent to the theoretical values 91.43% and 8.49%, respectively.

3.4. Luminescent Properties

The compounds $[Li(NPA)_2H_2O]$(1b) and $[Na(NPA)_2]$(2b) showed two strong fluorescence emissions (blue emission maxima) with greater intensity comparative to their ligand fluorescence emission i.e NPA.[50] While the compounds [Li(NPG)](1a), $[Na(NPG)_2]\cdot 2H_2O$(2a) showed two weak fluorescence emissions (blue emission maxima) with less intensity comparative to their ligand fluorescence emission i.e. NPG as shown in Fig.7.

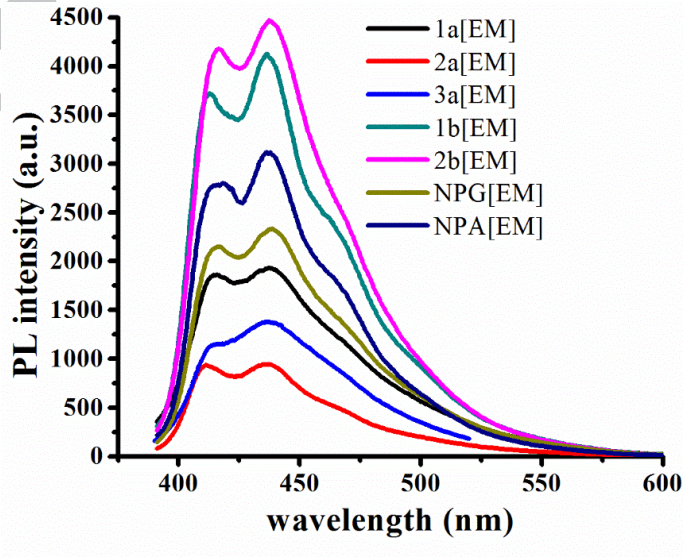

Fig. 7. Fluorescence spectrum of compounds in 1.0×10^{-3} M in DMSO solution at 25.0 ± 0.1 ºC.

Due to base hydrolysis of NPG for potassium complex $[C_8H_5KO_4]$(3a) [51] ligand based fluorochrome has been changed showing different shape of emission spectrum as compared to other compounds. Fluorescence emissions spectra depicted in Fig. 8 and data is presented in Table 7.

Table 7. Fluorescence data of compounds 1a, 2a, 3a, 1b, 2b NPG and NPA.

Compounds	EX(nm)	EM(nm)	Stoke Shift(nm)
1a	367	415 & 438	48 & 71
2a	367	411 & 437	44 & 70
3a	366	414 & 438	48 & 72
1b	374	413 & 437	39 & 63
2b	368	417& 438	49 & 70
NPG	364	417 & 438	53 & 74
NPA	368	417 & 439	49 & 71

Due to the resemblance in the shapes and positions of fluorescence emission and excitation pattern of complexes and ligands, it can be decided that the emissions observed for the complex is neither MLCT (metal-to-ligand charge transfer) nor LMCT (ligand-to-metal charge transfer) in nature, and can be assumed as the intra-ligand fluorescent emission. [52] The emission observed in the compounds assigned to the ($\pi\rightarrow\pi^*$ & $n\rightarrow\pi^*$) intra-ligand fluorescence. [53] The slight difference in the positions of luminescent peaks in the compounds may be due to the different coordination modes of ligands.

Conclusion

In this work, new polymeric nature compounds [Li(NPG)], $[Na(NPG)_2]\cdot 2H_2O$, $[C_8H_5KO_4]$, $[Na(NPA)_2]$ had been synthesized. These compounds are structurally characterized as thermally stable supramolecular alkali metal coordination polymers. The compound $[Li(NPA)\cdot H_2O]$ did not show self-assembly, so it can be regarded as lithium complex of NPA. Co-ordination geometries along with coordination modes were discussed. The coordination modes are verified by the utilization of useful information

provided by FTIR and Raman spectroscopies. The thermal stability data showed that the coordination polymers are stable up to much higher extent. Compounds 1a, 2a, 1b & 2b showed ligand-based photoluminescence properties while in the 3a, ligand based fluorochrome has been changed showing different shape of emission spectrum as compared to other compounds.

Supplementary Information

Crystallographic data (excluding structure factors) for the structures in this paper have been deposited in the Cambridge Crystallographic Data Centre as supplementary publication, CCDC Nos. 870359, 870722, 872685, 873800 and 876492 for compounds 1a, 2a, 3a, 1b and 2b respectively. Copies of the data can be obtained free of charge on application to CCDC, 12 Union Road, Cambridge CB2 1EZ, UK (fax: (internet) +44 1223 336 033; e-mail: deposit@ccdc.cam.ac.uk). or www at http://www.ccdc.cam.ac.uk].

References

[1] R. Murugavel, V.V. Karambelkar, G. Anantharaman, M.G. Walawalkar, Synthesis, Spectral Characterization, and Structural Studies of 2-Aminobenzoate Complexes of Divalent Alkaline Earth Metal Ions: X-ray Crystal Structures of $[Ca(2\text{-aba})_2(OH_2)_3]_\infty$,$[\{Sr(2\text{-aba})_2(OH_2)_2\}_\infty H_2O]_\infty$, and $[Ba(2\text{-aba})_2 (OH_2)]_\infty$(2-abaH= 2-$NH_2C_6H_4COOH$), Inorg. Chem. 39 (2000) 1381-1390.

[2] J. Lan, D. Cao, W. Wang, B. Smit, Doping of alkali, alkaline-earth, and transition metals in covalent-organic frameworks for enhancing CO_2 capture by first-principles calculations and molecular simulations, Acs Nano. 4 (2010) 4225-4237.

[3] J. Huskens, D. A. Torres, Z. Kovacs, J. P. André, C. F. Geraldes, A. D. Sherry, Alkaline earth metal and lanthanide (III) complexes of ligands based upon 1, 4, 7, 10-tetraazacyclododecane-1, 7-bis (acetic acid), Inorg. Chem. 36 (1997) 1495-1503.

[4] J. Sebastian, K.M. Jinka, R.V. Jasra, Effect of alkali and alkaline earth metal ions on the catalytic epoxidation of styrene with molecular oxygen using cobalt (II)-exchanged zeolite X, Jo Catal. 244 (2006) 208-218.

[5] M. Takagi, K. Ueno, Crown compounds as alkali and alkaline earth metal ion selective chromogenic reagents, Host Guest Complex Chemistry III, Springer. 121(1984) 39-65.

[6] H. Wu, W. Zhou, T. Yildirim, Alkali and alkaline-earth metal amidoboranes: structure, crystal chemistry, and hydrogen storage properties, J. Am. Chem. Soc. 130 (2008) 14834-14839.

[7] K. M. Fromm, R. D. Bergougnant, Transport properties of solid state crown ether channel systems, Solid. state. Sci. 9 (2007) 580-587.

[8] K. M. Fromm, Recent advances in the chemistry of clusters and inorganic polymers of alkali and alkaline earth metal compounds, Chimi. Int. J. Chem. 56 (2002) 676-680.

[9] K. M. Fromm, Coordination polymer networks with S-block metal ions, Coord. Chem. Rev. 252 (2008) 856-885.

[10] R. J. Kuppler, D. J. Timmons, Q. R. Fang, J. R. Li, T. A. Makal, M. D. Young, D. Yuan, D. Zhao, W. Zhuang, H. C. Zhou, Potential applications of metal-organic frameworks, Coord. Chem. Rev. 253 (2009) 3042-3066.

[11] M. Eddaoudi, D. B. Moler, H. Li, B. Chen, T. M. Reineke, M. O'keeffe, O. M. Yaghi, Modular chemistry: secondary building units as a basis for the design of highly porous and robust metal-organic carboxylate frameworks, Acc. Chem. Res. 34 (2001) 319-330.

[12] C. Rao, S. Natarajan, R. Vaidhyanathan, Metal carboxylates with open architectures, Ang. Chem. Int. Ed. 43 (2004) 1466-1496.

[13] M. P. Suh, Y. E. Cheon, E. Y. Lee, Syntheses and functions of porous metallosupramolecular networks, Coord. Chem. Rev. 252 (2008) 1007-1026.

[14] M. Yoshizawa, M. Nagao, K. Umemoto, K. Biradha, M. Fujita, S. Sakamoto, K. Yamaguchi, Side chain-directed assembly of triangular molecular panels into a tetrahedron vs. open cone, Chem. Commun. 0 (2003) 1808-1809.

[15] G. Dong, P. Ke-liang, D. Chun-ying, H. Cheng, M. Qing-jin, Design and Crystal Structures of Triple Helicates with Crystallographic Idealized D_3 Symmetry: The Role of Side Chain Effect on Crystal Packing, Inorg. Chem. 41 (2002) 5978-5985.

[16] X. L. Wang, Y. Q. Chen, G. C. Liu, H. Y. Lin, W. Y. Zheng, J. X. Zhang, Assembly of novel phenanthroline-based cobalt (II) coordination polymers by selecting dicarboxylate ligands with different spacer length: From 1-D chain to 3-D interpenetrated framework, J. Organomet. Chem. 694 (2009) 2263-2269.

[17] Y. Liu, Y. Qi, Y. H. Su, F. H. Zhao, Y. X. Che, J. M. Zheng, Five novel cobalt coordination polymers: effect of metal–ligand ratio and structure characteristics of flexible bis (imidazole) ligands, CrystEngComm, 12 (2010) 3283-3290.

[18] F. Y. Cui, K. L. Huang, Y. Q. Xu, Z. G. Han, X. Liu, Y. N. Chi, C. W. Hu, Structural variability of Cd (II) and Co (II) mixed-ligand coordination polymers: effect of ligand isomerism and metal-to-ligand ratio, CrystEngComm, 11 (2009) 2757-2769.

[19] B. C. Tzeng, H. T. Yeh, T. Y. Chang, G. H. Lee, Novel Coordinated-Solvent Induced Assembly of Cd (II) Coordination Polymers Containing 4, 4′-Dipyridylsulfide, Cryst. Growth Des. 9 (2009) 2552-2555.

[20] S. C. Chen, Z. H. Zhang, K. L. Huang, Q. Chen, M. Y. He, A. J. Cui, C. Li, Q. Liu, M. Du, Solvent-controlled assembly of manganese (II) tetrachloroterephthalates with 1D chain, 2D layer, and 3D coordination architectures, Cryst. Growth Des. 8 (2008) 3437-3445.

[21] T. Prasad, M. Rajasekharan, Solvent dependent crystallization of isomeric chain coordination polymers in the Ce-Zn/Cd-dipic system, Cryst. Growth Des. 8 (2008) 1346-1352.

[22] V. Pedireddi, S. Varughese, Solvent-dependent coordination polymers: Cobalt complexes of 3, 5-dinitrobenzoic acid and 3, 5-dinitro-4-methylbenzoic acid with 4, 4'-bipyrdine, Inorg. Chem. 43 (2004) 450-457.

[23] N. P. Chatterton, D. M. Goodgame, D. A. Grachvogel, I. Hussain, A. J. White, D. J. Williams, Influence of the Counteranion on the Formation of Polymeric Networks by Metal Complexes of Hexamethylenebis (acetamide), Inorg. Chem. 40 (2001) 312-317.

[24] H. Yoo, H. D. Mai, I. Lee, S. Lee, Alkali-Metal-Mediated Frameworks based on Di-(2, 6-Pyridinedicarboxyate) Cobalt (II) Species, Eur. J. Inorg. Chem, 31 (2017) 3736-3743.

[25] S. M. Humphrey, R. A. Mole, R. I. Thompson, P. T. Wood, Mixed Alkali Metal/Transition Metal Coordination Polymers with the Mellitic Acid Hexaanion: 2-Dimensional Hexagonal Magnetic Nets, Inorg. Chem. 49 (2010) 3441-3448.

[26] L. D. M. Lima, P. Castro, A. L. Machado, C. A. M. Fraga, C. Lugnier, V. L. G. de Moraes, E. J. Barreiro, Synthesis and anti-inflammatory activity of phthalimide derivatives, designed as new thalidomide analogues, Bioorganic Med. Chem. 10 (2002) 3067-3073.

[27] N. Barooah, J. B. Baruah, Supramolecular chemistry with phthalimide derivatives, Mini Rev. Org. Chem. 4 (2007) 292-309.

[28] Y. Chen, L. Deng, Parallel kinetic resolutions of monosubstituted succinic anhydrides catalyzed by a modified cinchona alkaloid, J. Am. Chem. Soc. 123 (2001) 11302-11303.

[29] M. E. Vázquez, J. B. Blanco, B. Imperiali, Photophysics and biological applications of the environment-sensitive fluorophore 6-N, N-dimethylamino-2, 3-naphthalimide, J. Am. Chem. Soc. 127 (2005) 1300-1306.

[30] C. J. McAdam, J. L. Morgan, R. E. Murray, B. H. Robinson, J. Simpson, Synthesis and fluorescence properties of new enaminenaphthalimides, Aust. J. Chem. 57 (2004) 525-530.

[31] T. Sakamoto, C. Pac, A "Green" Route to Perylene Dyes: Direct Coupling Reactions of 1, 8-Naphthalimide and Related Compounds under Mild Conditions Using a "New" Base Complex Reagent, t-BuOK/DBN, J. Org Chem, 66 (2001) 94-98.

[32] M. E. Vázquez, D. M. Rothman, B. Imperiali, A new environment-sensitive fluorescent amino acid for Fmoc-based solid phase peptide synthesis, Org. Biomol. Chem. 2 (2004) 1965-1966.

[33] S. F. Muhammed, Synthesis and Characterization of Some N-Protected Amino Acid Complexes, J. Am. Sci, 6 (2010).

[34] R. Antunes, H. Batista, R. Srivastava, G. Thomas, C. Araujo, New Phthalimide derivatives with potent analgesic activity: II, Bioorg. Med. Chem. Lett. 8 (1998) 3071-3076.

[35] N. Barooah, R. J. Sarma, A. S. Batsanov, J. B. Baruah, N-phthaloylglycinato complexes of Cobalt, Nickel, Copper and Zinc, Polyhedron. 25 (2006) 17-24.

[36] M. N. Khan, Suggested improvement in the ing-manske procedure and gabriel synthesis of primary amines: kinetic study on alkaline hydrolysis of N-phthaloylglycine and acid hydrolysis of N-(o-Carboxybenzoyl) glycine in aqueous organic solvents, J. Org. Chem, 61 (1996) 8063-8068.

[37] K. Nakamoto, Infrared and Raman spectra of inorganic and coordination compounds, Wiley Online Library1986.

[38] G. Kumar, M. Srivastava, Spectral and magnetochemical studies of nickel (II) and cobalt (II) complexes of hippuric acid, Rev Chim Miner. 16 (1979) 14-18.

[39] G. Socrates, Infrared and Raman characteristic group frequencies: tables and charts, John Wiley & Sons 2001.

[40] G. M. Sheldrick, A short history of SHELX, Acta Crystallogr. Sect. A: Found. Crystallogr. 64 (2007) 112-122.

[41] M. Dinca, J. R. Long, Strong H_2 binding and selective gas adsorption within the microporous coordination solid $Mg_3(O_2C\text{-}C_{10}H_6\text{-}CO_2)_3$, J. Am. Chem. Soc. 127 (2005) 9376-9377.

[42] J. Krogh-Moe, The crystal structure of lithium diborate, $Li_2O.\ 2B_2O_3$, Acta Crystallogra. 15 (1962) 190-193.

[43] M. G. Gardiner, G. R. Hanson, M. J. Henderson, F. C. Lee, C. L. Raston, Paramagnetic Bis (1, 4-di-tert-butyl-1, 4-diazabutadiene) Adducts of Lithium, Magnesium, and Zinc, Inorganic Chemistry, 33 (1994) 2456-2461.

[44] O. Yaghi, C. E. Davis, G. Li, H. Li, Selective guest binding by tailored channels in a 3-D porous zinc (II)-benzenetricarboxylate network, J. Am. Chem. Soc. 119 (1997) 2861-2868.

[45] W. L. Armarego, B. A. Milloy, W. Pendergast, A highly stereospecific synthesis of (R)-and (S)-[2-2 H 1] glycine, J. Chem. Soc. (1976) 2229-2237.

[46] T. Takahashi, T. Kikuchi, Porosity dependence on thermal diffusivity and thermal conductivity of lithium oxide Li_2O from 200 to 900° C, J. Nucl. Mater. 91 (1980) 93-102.

[47] J. Scheirs, G. Camino, W. Tumiatti, Overview of water evolution during the thermal degradation of cellulose, Euro. Poly. J, 37 (2001) 933-942.

[48] A. Petrocelli, D. Kraus, The inorganic superoxides, J. Chem. Edu. 40 (1963) 146.

[49] I. Hickman, J. Jonsson, J. Prins, S. Ash, D. Purdie, A. Clouston, E. Powell, Modest weight loss and physical activity in overweight patients with chronic liver disease results in sustained

improvements in alanine aminotransferase, fasting insulin, and quality of life, Gut. 53 (2004) 413-419.

[50] F. Brun, J. J. Toulme, C. Helene, Interactions of aromatic residues of proteins with nucleic acids. Fluorescence studies of the binding of oligopeptides containing tryptophan and tyrosine residues to polynucleotides, Biochemistry. 14 (1975) 558-563.

[51] D. J. Jobe, R. E. Verrall, R. Palepu, V. C. Reinsborough, Fluorescence and conductometric studies of potassium 2-(p-Toluidinyl) naphthalene-6-sulfonate/Cyclodextrin/Surfactant systems, J. Phy. Chem. C. 92 (1988) 3582-3586.

[52] X. Meng, H. Hou, G. Li, B. Ye, T. Ge, Y. Fan, Y. Zhu, H. Sakiyama, Tetrametallic macrocyclic frameworks constructed from ferrocenedicarboxylato and 2, 2′-bipyridine: synthesis, molecular structures and characteristics, J. Organomet. Chem. 689 (2004) 1218-1229.

[53] Y. M. Cheng, Y. S. Yeh, M. L. Ho, P. T. Chou, P. S. Chen, Y. Chi, Dual room-temperature fluorescent and phosphorescent emission in 8-quinolinolate osmium (II) carbonyl complexes: Rationalization and generalization of intersystem crossing dynamics, Inorg. Chem. 44 (2005) 4594-4603.

Research Highlights

- Synthesis of five alkali metal coordination compounds has been performed.
- Hydrolysis of N-phthaloyl glycine, resulted, the formation of potassium compound with phthalic acid [$C_8H_5KO_4$].
- Different carboxylate coordination modes $\eta^2\mu^3$and $\eta^1\mu^1$ $\eta^2\mu^2$ with interesting geometries around alkali metals.
- Thermal stability studies of alkali metal coordination compounds have been carried out.
- Lithium and sodium compounds of N-phthaloyl-ß-alanine showed two strong fluorescence emissions enhancement relative to their ligand.